Engineering 25 (2023) 157–167

Contents lists available at ScienceDirect

Engineering

journal homepage: www.elsevier.com/locate/eng

Research
Green Chemical Engineering—Article

Flow-Electrode Microbial Electrosynthesis for Increasing Production Rates and Lowering Energy Consumption

Na Chu [a,b], Donglin Wang [c], Houfeng Wang [a], Qinjun Liang [a], Jiali Chang [d], Yu Gao [a], Yong Jiang [a,*], Raymond Jianxiong Zeng [a]

[a] Fujian Provincial Key Laboratory of Soil Environmental Health and Regulation, College of Resources and Environment, Fujian Agriculture and Forestry University, Fuzhou 350002, China
[b] CAS Key Laboratory of Environmental and Applied Microbiology, Environmental Microbiology Key Laboratory of Sichuan Province, Chengdu Institute of Biology, Chinese Academy of Sciences, Chengdu 610041, China
[c] State Key Laboratory of Environmental Aquatic Chemistry, Research Center for Eco-Environmental Sciences, Chinese Academy of Sciences, Beijing 100085, China
[d] Division of Environmental Engineering, School of Chemistry, Resources and Environment, Leshan Normal University, Leshan 614000, China

ARTICLE INFO

Article history:
Received 5 June 2021
Revised 8 September 2021
Accepted 14 September 2021
Available online 15 December 2021

Keywords:
CO_2 utilization
Biocathode
Transcriptional analysis
Microbial electrochemical technology
Extracellular electron transfer

ABSTRACT

The development of microbial electrosynthesis (MES) for renewable electricity-driven bioutilization of CO_2 has recently attracted considerable interest due to its ability to synthesize chemicals with the transition towards a circular carbon economy. However, the increase of acetate production and the decrease of energy consumption of MES using an advanced reactor design have received less attention. In this study, the total acetate production rate using novel flow-electrode MES reactors ((16 ± 1) $g \cdot m^{-2} \cdot d^{-1}$) was double that using reactors without powder activated carbon (PAC) amendment ((8 ± 3) $g \cdot m^{-2} \cdot d^{-1}$). The flow-electrode MES reactors had a Coulombic efficiency of 43.5% ± 3.1%, an energy consumption of (0.020 ± 0.005) $kW \cdot h \cdot g^{-1}$, and an energy efficiency of 18.7% ± 1.3% during acetate production. The flow-electrode with PAC amendment could decrease the net water flux and charge transfer resistance, while had little impact on the cell voltage, rheological behavior, and acetate adsorption. In the flow-electrode MES reactors, the expression of genes involving in energy production and conversion were increased, and the increase of acetate production was found correlated with the increased abundance of *Acetobacterium*. The Wood–Ljungdahl pathway (WLP) and reductive citric acid cycle (rTCA) were found to be the pathways responsible for carbon fixation. The concentrations of acetate in the stacked flow-electrode MES reached 7.0 $g \cdot L^{-1}$. This study presents a new approach for the construction of scalable MES reactors with high-performance chemical generation and CO_2 utilization.

1. Introduction

Rapid urbanization and population growth have impacted the environment in many ways, including the emission of greenhouse gas (e.g., CO_2) [1–3]. The application of current technologically viable methods for CO_2 capture and sequestration to reduce CO_2 emissions is restricted by their high costs with low intrinsic value of CO_2 [4]. The development of thermochemical, electrochemical, and bioelectrochemical approaches for CO_2 utilization has recently attracted increasing attention due to the transition towards a circular carbon economy [5,6].

Microbial electrosynthesis (MES) is a technique that uses microbes as biocatalysts to produce valuable chemicals driven by electrical energy [7]. Owing to its advantages including low-cost biocatalysts, low overpotential, and mild operating conditions, MES has attracted increasing attention from researchers in different disciplines during the past decade. Much effort has been made to promote the acetate production using MES as it has high selectivity [8], and the acetate produced can be extracted on-line [9], which is beneficial in avoiding the problem of potential product inhibition [10]. With the bioconversion of acetate as an intermediate compound, MES can be integrated with other existing biorefinery technologies to produce high value-added chemicals such as medium-chain fatty acids, proteins, and bioplastics [11–13].

From the engineering point of view, the inward extracellular electron transfer from cathodes to microbes in MES is

* Corresponding author.
E-mail address: jiangyongchange@163.com (Y. Jiang).

https://doi.org/10.1016/j.eng.2021.09.015

surface-dependent, whereas the efficiency of chemical accumulation is volume-dependent [14]. Thus, the scale up of MES reactors is difficult and can be significantly different from the classic biochemical reactors. During the last decade, efforts have been made to increase the inward extracellular electron transfer, which can include the use of nanomaterials that have improved biological compatibility and the selection of microbes that have accelerated autotrophic metabolisms [11,12]. In addition, three-dimensional (3D) material-based cathodes and packed-bed cathodes have also been used in MES to increase the volume-dependent chemical production [14]; however, these cathodes have some associated problems including hardness, conductivity, biofilm obstruction, and redox potential heterogeneity [15,16]. Due to these limitations, much less effort has been put on the scalable reactor design, and almost 70% of MES studies in the past decade used conventional H-type reactors [17].

Flow-electrode-based electrochemical reactors can be constructed using a liquid-type flow-electrode that is separated from the electrochemical cells. These reactors are different from the conventional reactors, which use solid-type electrodes fixed in the electrochemical cells [18]. The flow-electrode can provide a charge transfer from a current collector to the conductive particles by constantly making and breaking contacts with each other of these particles, which thus allowing the electrode surface area to increase independently with the volume of the electrochemical reactors [19]. For example, flow-electrode capacitive deionization (FCDI) has been used for desalination and nutrient recovery [20]. Increasing the electrode surface area independently of the volume of a MES reactor is a key issue that needs to be overcome, as the electron consumption rate of biofilm with a low thickness is generally insufficient to meet the high current density needed for most practical applications [21]. It should be noted that the term "flow-through double carbon felt cathode" has been applied to the cathode made of carbon felt with catholyte flowing through it [22], and the term is different from the term "flow-electrode," which refers to flowable particle electrodes, used in the present study [20]. Despite the lack of experimental evidence, it may be possible to introduce the flow-electrode into MES bioreactors to increase the area of surface for attachment of biofilm and bioutilization of CO_2, as well as to direct electron and carbon fluxes.

In this study, a novel MES reactor configured with a flow-electrode was assembled for the first time to enhance chemical production and decrease energy consumption. The performance of the flow-electrode MES reactors including chemical production, Coulombic efficiency (CE), energy recovery, and electrochemical characteristics were evaluated and compared with those of the reactors without powder activated carbon (PAC). Transcriptional analysis was performed to examine the electron and carbon fluxes. In addition, the performance of stacked flow-electrode MES reactors was evaluated. The use of flow-electrode is a new approach that can be employed in the construction of high performance and scalable MES reactors.

2. Materials and methods

2.1. Reactor configuration and operation

Four MES devices with the same structure and size were assembled and divided into two groups: flow-electrode MES reactors and reactors without PAC. In the flow-electrode MES reactors (Fig. 1), the catholyte was amended with 2.0 $g \cdot L^{-1}$ of PAC (YEC-200D, Yihuan Carbon Co., Ltd., China) with an average particle diameter of 20 μm and a specific surface area of 2013 $m^2 \cdot g^{-1}$. The total surface area of the cathode, which is contributed mainly by the PAC rather than the channels on graphite sheet, was calculated to be 402.6 m^2. The concentration of PAC was selected based on our previous studies [9], in which higher concentrations of PAC were found to inhibit the bioactivity. Titanium mesh coated with iridium and ruthenium (6 cm × 6 cm × 0.1 cm; Mingxuan Metallic Material Co., Ltd., China) was used as the anode for the oxygen evolution reaction (OER). The extraction chamber consisted of two pieces of silicone gaskets and a piece of 0.9 mm thick nylon grid that lied between a pair of ion exchange membranes, a cation exchange membrane (CEM) and an anion exchange membrane (AEM) (3361BW; Shanghai Shanghua Water Treatment Materials Co., Ltd., China). Acetate produced from CO_2 in an anionic form was allowed to cross the AEM during its migration from the cathodic chamber to the extraction chamber [23]. Both the anodic and cathodic chambers were constructed based on hollow serpentine channels carved into a conductive graphite sheet (details of the pattern are provided in Fig. S1 in Appendix A)). The channels were 2 mm in width and 2 mm in depth; thus, the projected surface area of the channels was 11.92 cm^2 [24]. The current collectors attached on the anodic and cathodic graphite sheets were made of titanium sheets (1 cm × 5 cm × 0.003 cm). A photograph of the flow-electrode MES reactor is provided (Fig. S2 in Appendix A). In addition, H-type MES reactors with the cathode made of carbon felt (CF) and multi-working electrode (WE) reactors with the cathode made of graphite sheet were constructed and used as the biotic controls. The abiotic control was conducted without microbial inoculation.

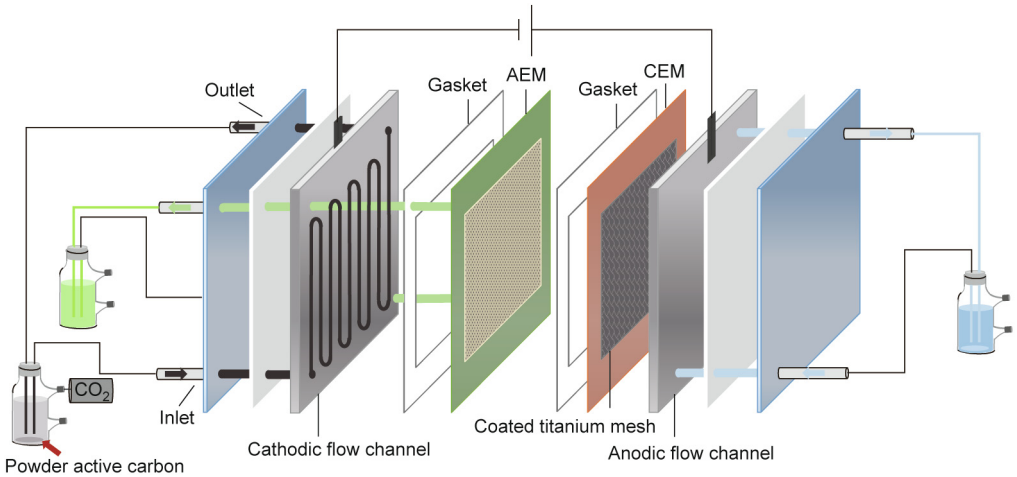

Fig. 1. Schematic illustration of the flow-electrode MES reactor constructed and used in this study. AEM: anion exchange membrane; CEM: cation exchange membrane.

The catholyte was prepared by mixing the following components: K_2HPO_4, 2.6 g·L^{-1}; KH_2PO_4, 4.4 g·L^{-1}; NH_4Cl, 0.31 g·L^{-1}; Na_2SO_4, 0.05 g·L^{-1}; $MgCl_2·6H_2O$, 0.2 g·L^{-1}; yeast extract, 0.05 g·L^{-1}; $NaHCO_3$, 4.2 g·L^{-1}, and 2-bromoethanesulfonate, 1.0 g·L^{-1}. The anolyte and extraction solution were prepared from the following components: K_2HPO_4, 2.6 g·L^{-1} and KH_2PO_4, 4.4 g·L^{-1}. Each of the catholyte, anolyte, and extraction solution at an equal volume (100 mL) was placed in three separated bottles. The catholyte and extraction solution were purged with N_2 gas for 15 min to create an anaerobic condition. The bottle containing the catholyte was connected to a gas bag with a volume of 1 L to allow the passive supplement of CO_2. The catholyte was inoculated with activated sludge after being cleaned three times [25]. The flow rate of the catholyte, anolyte, and extraction solution was fixed at (1.3 ± 0.1) mL·min^{-1} and controlled using a multichannel peristaltic pump (BT100-1L; Baoding Longer Precision Pump Co., Ltd., China). The flow rate was selected to ensure that the flow electrode could be smoothly pumped into and out of the reactors. The effect of flow rate (the values for catholyte, anolyte, and extraction solution were different) on the performance of the flow-electrode MES reactor need to be further explored. The MES reactors were run under galvanostatic mode, which is the mode that allows the use of low-cost electronic periphery in a straightforward two-electrode arrangement [26–28]. The cell voltage was recorded because the cathodic potential could not be directly measured as the conventional reference electrode could not be inserted into reactors. The current was fixed at 1, 3, and 6 mA, each was maintained for 12 d [29]. The product accumulation and cell voltage were stable after 12 d at each of the fixed current value. The use of low fixed current during the startup time was to prevent a dramatically increase of pH due to the fast generation of hydrogen. In addition, the performance of stacked flow-electrode MES reactors was evaluated. The reactors were operated at room temperature, and the reported data were average values from duplicate experimental set-ups.

2.2. Analyses and calculations

The voltage and current of the MES reactors, operated under galvanostatic mode, were recorded using a battery testing system (CT-4008; Neware Technology Co., Ltd., China). The catholyte, anolyte, and extraction solution samples were analyzed using a gas chromatograph (GC) equipped with a flame ionization detector (FID) (Nexis GC-2030; Shimadzu Corporation, Japan), in which potential products including acetate, propionate, isobutyrate, butyrate, isovalerate, and butanol were detected. Gas components were analyzed using a GC equipped with a thermal conductivity detector (TCD) (SP 6890; Lunan Inc., China).

The production rate was normalized to the projected surface area of the channels on the graphite sheet (11.92 cm^2). The equilibrium sorption capacity of PAC dissolved in the catholyte was calculated using a method described in a previous study [30]. The rheological properties of electrolyte with and without PAC amendment were evaluated using a hybrid rheometer (Discovery HR-1; TA Instruments, USA); the shear rate was increased logarithmically from 0.01 to 500 s^{-1} in the steady shear mode [31].

Electrochemical impedance spectroscopy (EIS) of the MES reactors was conducted using an electrochemical workstation (660E; CH Instruments, USA), in which the cathode served as the working electrode, while the anode served as the counter electrode. The frequency range was 100 000 to 0.010 Hz with a voltage amplitude of 10 mV and a cell voltage of 0 V. EIS and cyclic voltammetry (CV) of the catholyte with and without PAC amendment were conducted in a single-chamber cell containing hollow serpentine channels to evaluate the effect of PAC on the electrochemical characteristics [32]. The anion crossover comparison was conducted abiotically in the H-type cells. The CE, which reflects the electron recovery, was calculated using different molar conversion factors for the identified products [33].

The energy consumption was calculated by Eq. (1):

$$\text{Energy consumption} = \frac{UIt}{(C_t - C_0) \times V} \quad (1)$$

where U is the cell voltage (V), I is the fixed current (A), t is the process time (s), C is the concentration of identified products (g·L^{-1}), and V is the volume of the electrolyte (L).

The energy efficiency was calculated from the higher heating value (HHV) of products divided by electrical energy consumed by the reactors according to Eq. (2) [34]:

$$\text{Energy efficiency} = \frac{(C_t - C_0) \times \text{HHV} \times V}{UIt} \times 100\% \quad (2)$$

The microbes that were enriched on PAC in the flow-electrode MES reactor amended with powder active carbon (AC1), in the catholyte of reactors without PAC, or on the carbon felt in the H-type MES reactors (CF1) were sampled using E.Z.N.A.® Soil RNA Midi Kit (Omega Bio-tek, USA). Because the amount of biomass was limited, the samples from the duplicate experimental set-ups were mixed before being subjected to RNA extraction for transcriptional analysis [35]. However, the reactors without PAC failed to provide a sufficient amount of RNA. Ribosomal RNAs (rRNAs) were eliminated using Ribo-Zero Magnetic kit (Epicentre, USA). RNA-Seq libraries were constructed using TruSeq™ RNA Sample Prep Kit (Illumina, USA) and were sequenced using a commercial Illumina HiSeq X Ten instrument (Majorbio Bio-pharm Technology Co., Ltd., China). The RNA-Seq reads were analyzed using CLC Genomics Workbench 6.5.1 software (Qiagen, Germany). After trimming low quality reads, rRNA was removed using SortMeRNA algorithms. The selected assembled contigs (≥ 500 base pairs (bp)) were used to predict the open reading frames (ORFs) on Prodigal (v2.6.3) [36], and ORFs < 100 bp were filtered out. All the predicted ORFs were merged and clustered using CD-HIT (v4.7); after that, they were used to construct a non-redundant gene library, which yielded a total of 62 862 ORFs [37]. Protein sequences of the non-redundant genes were blasted against the National Center for Biotechnology Information (NCBI)-Non-Redundant (NR) Protein Sequence Database using DIAMOND (v0.8.12) to obtain species annotation. Functional annotation was obtained using eggNOG [38]. BBmap (v0.43.1) was used to map the clean reads into the non-redundant gene library to obtain gene abundance data. The results were manually curated with the fold change ≥ 5.

3. Results and discussion

3.1. Influence of PAC amendment on chemical production

The chemicals accumulated over time in the catholyte, extraction solution, and anolyte in both types of reactors were monitored (Fig. 2). Acetate was detected in the catholyte on day 6, indicating that the microbes underwent an adaptation stage to adapt to the electrochemical reactors, which is in agreement with the finding reported in previous studies [39,40]. The acetate production rate in the catholyte increased with the increase of fixed current (Figs. 2(a) and (b)). As the current was increased to 6 mA, the acetate production rate in the catholyte increased to (5.5 ± 0.5) g·m^{-2}·d^{-1} in the flow-electrode MES reactors and to (4.7 ± 1.5) g·m^{-2}·d^{-1} in the reactors without PAC. The acetate accumulation rate in the extraction solution also increased with the increase of electric current. As the current was increased to 6 mA, the acetate accumulation rate in the extraction solution increased to (8.6 ± 0.1) g·m^{-2}·d^{-1} in the flow-electrode MES reactors and to (2.7 ± 1.3) g·m^{-2}·d^{-1} in the reactors without PAC. Acetate was detected in

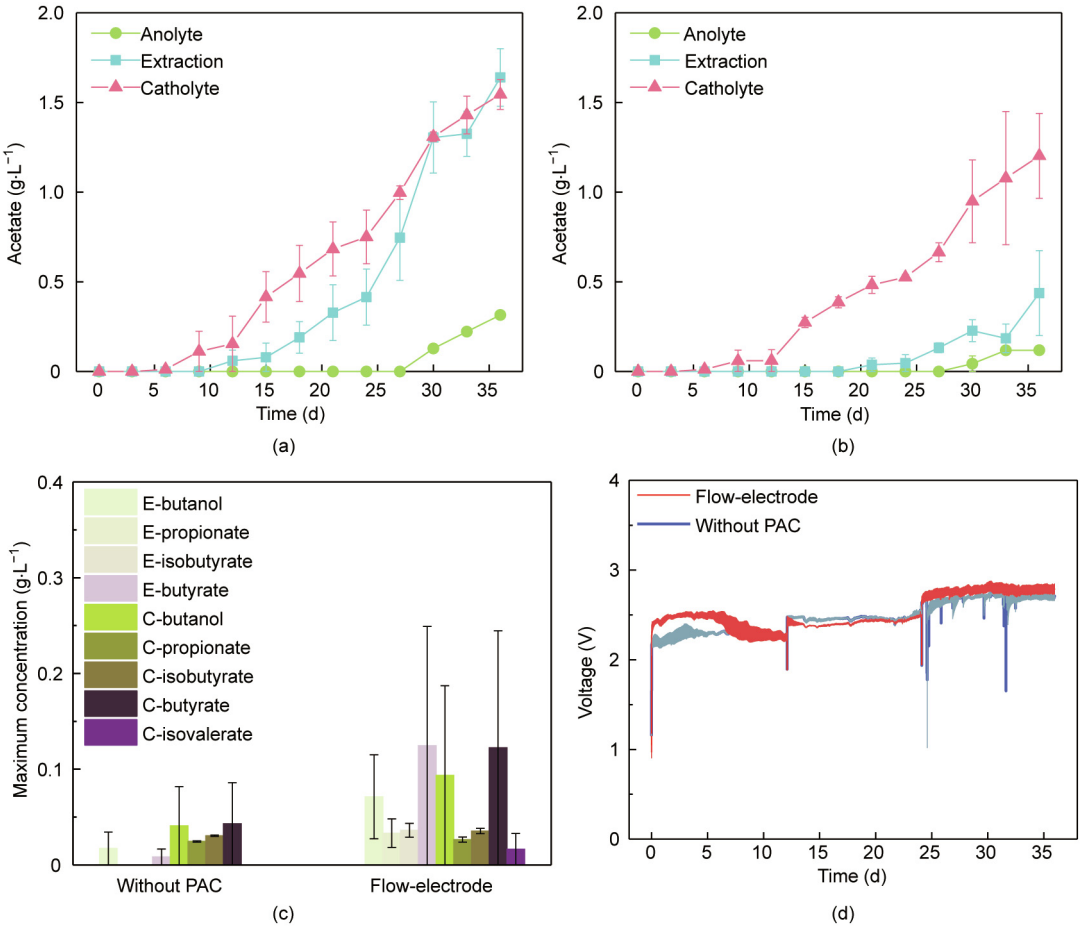

Fig. 2. Time course of acetate production in (a) the flow-electrode MES reactors and (b) the reactors without PAC. (c) Maximum concentrations of soluble by-products. (d) Change of cell voltage over time. The current was first fixed at 1 mA, followed by 3 and 6 mA, each for a period of 12 days. E: extraction. C: catholyte. Symbols in (a) and (b) and bars in (c) represent the average values from duplicate experimental set-ups, and error bars represent their ranges.

the anolyte with a maximum concentration of (0.31 ± 0.01) g·L^{-1} in the flow-electrode MES reactors and of (0.12 ± 0.02) g·L^{-1} in the reactors without PAC. The diffusion of the uncharged acetic acid from the CEM towards the anolyte has also been observed in previous studies [41]. Collectively, the total acetate production rate was (16 ± 1) g·m^{-2}·d^{-1} in the flow-electrode MES reactors and (8 ± 3) g·m^{-2}·d^{-1} in the reactors without PAC.

Acetate was not detected in the abiotic control (Fig. S3 in Appendix A). The acetate production performance of the H-type MES reactors (Fig. S4 in Appendix A) and the multi-WE reactors (Fig. S5 in Appendix A) developed in the present study was comparable to that reported in previous studies [42,43]. The acetate production rate of the flow-electrode MES reactors was much higher than that of the multi-WE reactors while was similar to that of the H-type MES reactors (Fig. S6 in Appendix A). The energy consumption required during acetate production was (0.020 ± 0.005) kW·h·g^{-1} for the flow-electrode MES reactors and was (0.04 ± 0.01) kW·h·g^{-1} for the reactors without PAC. It should be noted that the energy consumption of the flow-electrode MES reactors during acetate production was only half that of the H-type MES reactors and was a quarter of that of the multi-WE reactors (Fig. S6 in Appendix A).

The acetate production rates of the flow-electrode MES reactors developed in the present study ((16 ± 1) g·m^{-2}·d^{-1}) were much higher than those reported in previous studies (0.06–2.00 g·m^{-2}·d^{-1}), in which nonporous bulk electrodes (e.g., graphite plate, carbon plate, or graphite stick) were used. The production rates obtained in this study were comparable to those obtained by previous studies, in which fiber-based electrodes (e.g., carbon felt and graphite felt) were used [44–47], but were slightly lower than those obtained by surface modification [48]. It should be noted that the acetate production rates presented in the present study are still an order of magnitude lower than those obtained using MES equipped with 3D nanometer-material decorated cathodes, after the rates were normalized to the projected surface area of cathode. For example, the highest acetate production rate ever obtained in MES is 685 g·m^{-2}·d^{-1}, and this is the result of using grown multiwalled carbon nanotubes (MWCNT) on reticulated vitreous carbon (RVC) [49]. In addition, an acetate production rate calculated from the linear-sweep voltammetry (LSV) test is 1330 g·m^{-2}·d^{-1}, which may be the overvaluation of its performance under unsteady state due to the capacitive property of the RVC with MWCNT deposit [50].

By-products including butanol, propionate, isobutyrate, butyrate, and isovalerate were also detected with the maximum concentrations below 0.3 g·L^{-1} in the catholyte and extraction solution (Fig. 2(c)). The time course of by-products production is presented (Fig. S7 in Appendix A). The production of soluble by-products from CO_2 in MES has been previously reported [11,27,51], and this occurrence may probably be due to the generation of acetyl-coenzyme A (the key intermediate for bioconversion) by microbes [44]. The use of the flow-electrode with PAC amendment had little impact on the cell voltage of the MES reactors (Fig. 2(d)). As the current was increased to 6 mA,

the cell voltage increased to (2.8 ± 0.1) V in the flow-electrode MES reactors and to (2.7 ± 0.1) V in the reactors without PAC.

3.2. CO_2 utilization and pH fluctuation

The production and consumption of gas are shown in Figs. 3(a) and (b). The CO_2 utilization rate increased over time with the maximum value of (137 ± 1) mL·d^{-1} in the flow-electrode MES reactors and (126 ± 5) mL·d^{-1} in the reactors without PAC. Trace amounts of methane were generated at rates of less than 1 mL·d^{-1} upon the addition of 2-bromoethanesulfonate, a methanogenic inhibitor [52]. Thus, the formation of hydrocarbonate and/or carbonate could, to a certain extent, contribute to the utilization of CO_2. When the current was increased to 6 mA, H_2 was detected in the reactors without PAC at a rate of (18 ± 12) mL·d^{-1}, which was much higher than that in the flow-electrode MES reactors (below 0.6 mL·d^{-1}). The *in-situ* generation and consumption of H_2 has been suggested to play important roles in the inward extracellular electron transfer in MES [40,44]. Hydrogen generated in the cathode chamber of MES can come from electrochemical or microbial sources. Graphite-based cathodic flow channels and PAC-based flow electrodes are not good catalysts for hydrogen generation [53]. However, the enriched biofilm on biocathodes and the particles synthesized by bacteria can contribute to hydrogen production and is believed to be the dominant source of hydrogen in MES reactors. The significant accumulation of H_2 in the reactors without PAC indicated that the bioactivity in the flow-electrode MES reactors was much higher than that in the reactors without PAC. The time course of gas composition is provided (Fig. S8 in Appendix A).

During the operation of both types of reactors, the pH of the catholyte initially increased slightly to 7.7 ± 0.1 and then stabilized at 7.3 ± 0.2 (Figs. 3(c) and (d)). The pH of the anolyte in both types of reactors initially decreased sharply from 6.5 ± 0.1 to 3.2 ± 0.2 during the first three days and then decreased steeply with increasing current before finally stabilized at 2.2 ± 0.2. The pH of the extraction solution was stable at about 6.4 ± 0.3 at a current of 1 mA during the initial 12 days for both types of reactors. When the current was increased to 6 mA, the pH of the extraction solution deceased rapidly to 3.0 ± 0.5 in the flow-electrode MES reactors and to 4.1 ± 0.6 in the reactors without PAC. It has previously been reported that MES reactors can be operated with the catholyte pH between 4.4 and 10 [12]. The hydrogen evolution reaction (HER) can increase the pH through the consumption of protons [54], while the generation of carboxylates helps to decrease the pH [11]. Here, both the low pH of the extraction solution in the AEM separated chamber and the accumulation of acetic acid may contribute to the decrease of the catholyte pH. These results suggest that a dynamic equilibrium of pH was achieved in the flow-electrode MES reactors.

3.3. Coulombs and energy recovery

The Coulombs/energy input and recovery are shown in Fig. 4. The Coulombs input into the reactors operated under galvanostatic mode was increased as the fixed current was increased. The Coulombs and energy recovery in the catholyte, extraction solution, and anolyte took place mostly as acetate, and a very small proportion of the recovery was the results of other soluble by-products. For example, the Coulombic efficiency of acetate and total soluble chemicals in the flow-electrode MES reactors were 43.5% ± 3.1% and 50.8% ± 8.4%, respectively, whereas those for the reactors without PAC were 21.8% ± 6.1% and 23.4% ± 6.7%, respectively. The energy efficiency for acetate production was

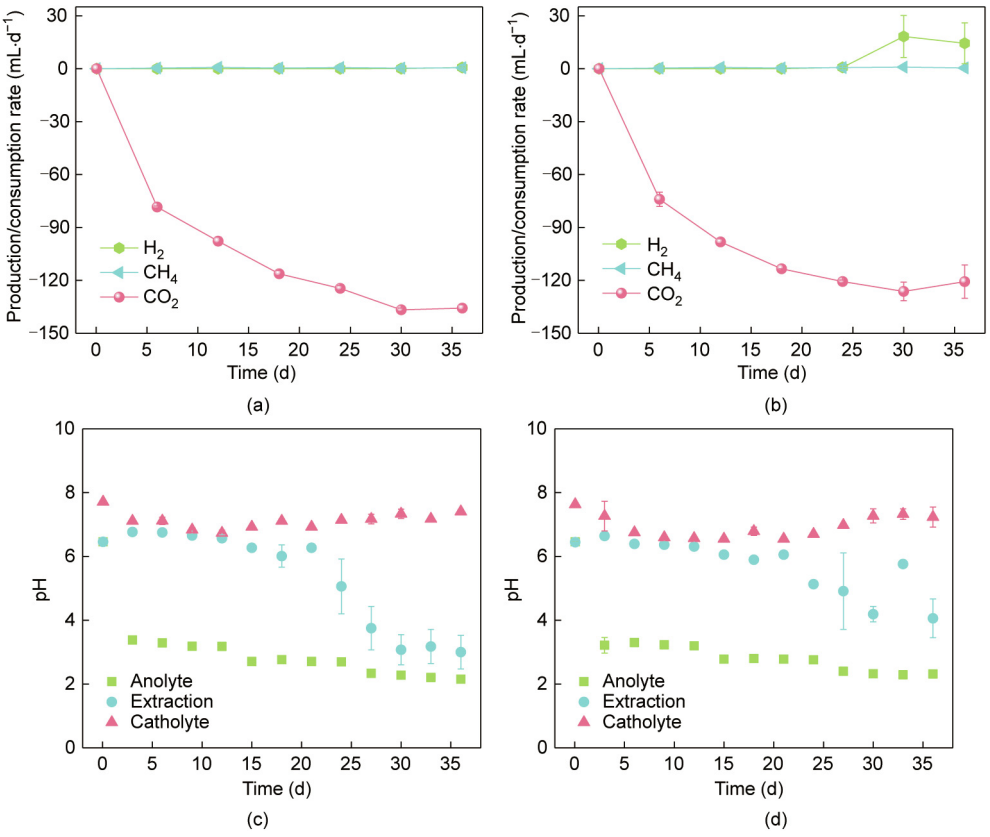

Fig. 3. Net production and consumption of gas in (a) the flow-electrode MES reactors and (b) the reactors without PAC. The pH fluctuation in (c) the flow-electrode MES reactors and (d) the reactors without PAC. Symbols represent the average values from duplicate experimental set-ups, and error bars represent their ranges.

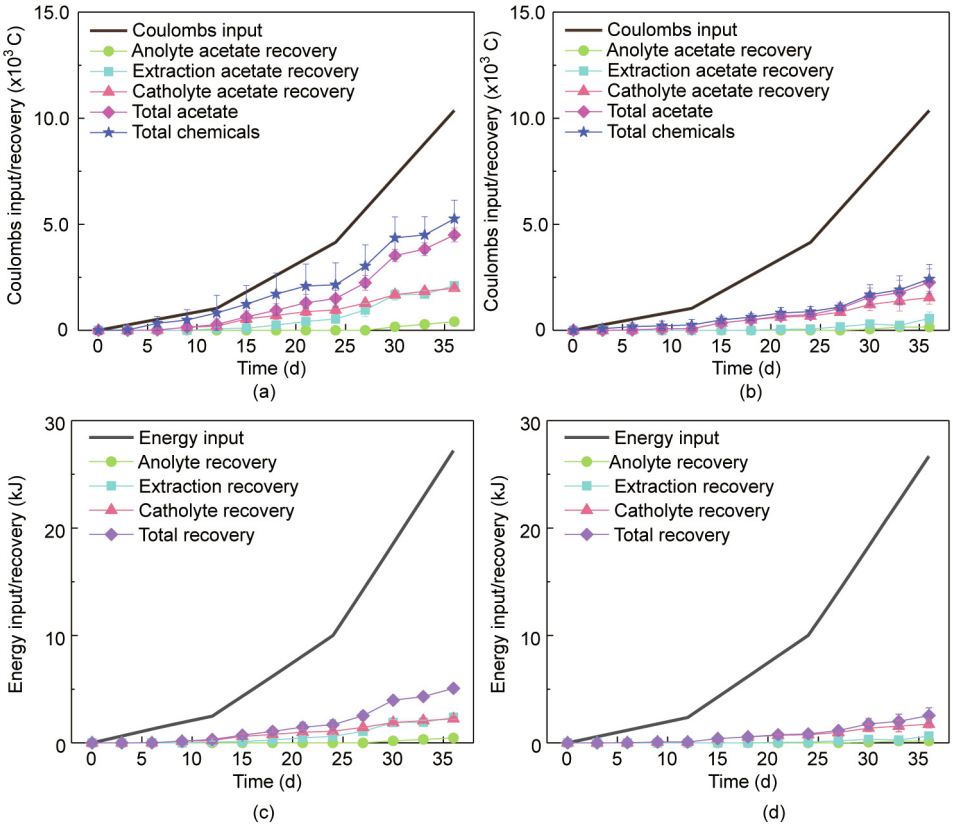

Fig. 4. Coulombs input/recovery (a) in the flow-electrode MES reactors and (b) in the reactors without PAC. Energy input and recovery (c) in the flow-electrode MES reactors and (d) in the reactors without PAC. Symbols represent the average values from duplicate experimental set-ups, and error bars represent their ranges.

18.7% ± 1.3% in the flow-electrode MES reactors and 9.6% ± 2.7% in the reactors without PAC.

Varying values of Coulombic efficiency from nearly 0 to almost 100% have been reported in previous studies using mixed-culture based MES reactors [8,44]. In these studies, the decrease of the Coulombic efficiency was found associated with the low electrochemical activity or low bioconversion of hydrogen *in situ*, as well as the consumption by heterotrophic bacterium. A recent review paper has described that almost 70% of MES studies in the past decade used the conventional H-type reactors [17]. High cell voltage is generally required in the H-type reactors due to large internal resistance caused by long electrode distances and small ion exchange membrane areas. For example, the energy recovery for acetate production of a previous study using H-type reactors was as low as 4.7%, and the cell voltage was as high as 3.8 V [39]. The energy recovery achieved in the present study (18.7% ± 1.3%) is higher than that achieved by a benchmark study, in which modular MES reactors and RVC foam-based cathodes were used and the achieved energy recovery was 12.1% [34].

3.4. Effects of PAC on the electrochemical characteristics

The effects of PAC on the electrochemical characteristics of the MES reactors were analyzed. The amendment with PAC remarkably decreased the net water flux rate (Fig. 5). For instance, the net water flux was not observed in the flow-electrode MES reactors when the current was fixed at 1 or 3 mA. When the current was increased to 6 mA, the net water flux between the extraction solution and the catholyte was at a rate of (2.7 ± 0.6) mL·d^{-1}. By contrast, in the reactors without PAC, the net water flux decreased with increasing current. For example, the net water flux in the reactors without PAC was (14.4 ± 6.5) mL·d^{-1} at 1 mA and was decreased to (7.3 ± 5.6) mL·d^{-1} at 6 mA. The net water flux, which is the combined results of electroosmosis and back-diffusion through membrane, can be affected by the types of separators, the properties of electrolyte solutions, and the operational parameters [9,55]. The amendment with PAC slightly decreased the crossover between inorganic anions (e.g., nitrate) and organic anions (e.g., acetate) (Fig. S9 in Appendix A). In addition, it increased the capacitance (see the CV plots) while decreased the resistance (see the EIS plots). Together, it may conclude that the decrease of the net water flux in the flow-electrode MES reactors was due to the decrease of anion crossover, increase of capacitance, and the decrease of resistance of the catholyte.

The amendment with PAC had little impact on the rheological behavior of the abiotic electrolyte, while the enrichment of microbes slightly increased the viscosity. The non-Newtonian characteristics and shear-thinning behavior of the catholyte were also observed. The PAC amendment with the enriched cathodic microbes remarkably decreased the internal resistance of the flow-electrode MES reactors, particularly for the charge transfer resistance, as indicated by the EIS (Fig. 5(d)). Previous studies have indicated that filling abiotic electrochemical reactors with conductive materials can promote ion transport [56]. However, the cell voltage of the flow-electrode MES reactors was not decreased due to the PAC amendment, which is probably because the ionic resistance could not contribute significantly to the internal resistance [57], as the ion strengths in both types of reactors were high. The contribution of acetate adsorption by PAC to the loss of Coulombs and energy recovery was limited, as the equilibrium solid-phase acetate concentration was below 0.02 mg·g^{-1} (Fig. S10 in Appendix A). It should be noted that the acetate

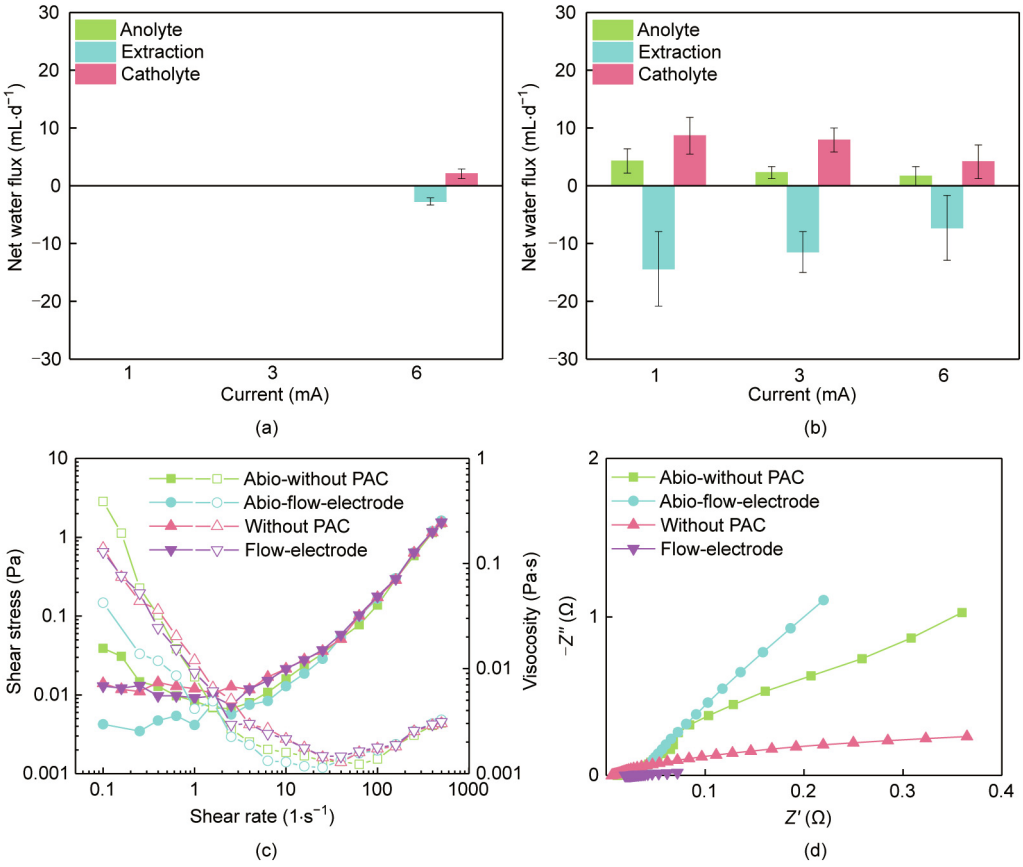

Fig. 5. Net water flux rate in (a) the flow-electrode MES reactors and (b) the reactors without PAC (bars are the average values from duplicate experimental set-ups, and error bars represent their ranges). (c) Rheological behavior of the electrolyte: solid symbols represent shear stress and open symbols viscosity. (d) Electrochemical impedance spectra of the MES reactors.

adsorption was limited because the concentration of PAC in the flow-electrode MES reactors was at least one order of magnitude lower than that in the flow-electrode capacitive deionization [20].

Collectively, these results indicate that the use of PAC amendment as the flow-electrode can promote the performance of MES reactors by decreasing the net water flux rate and the charge transfer resistance, and the use has little impact on the rheological behavior or the adsorption of products. As a proof-of-concept, in the present study, acetate was produced from the bioconversion of CO_2. The product spectrum of the flow-electrode MES reactors can potentially be expanded using strategies that can lead to metabolic shifts, for example, by using novel microbes as the biocatalyst [58], integrated process design [59], co-valorization with organic waste [39], and parameter optimization [60].

3.5. Transcriptional analysis

Acetobacterium (41.7% in AC1 and 24.94% in CF1) and *Wolinella* (27.96% in AC1 and 13.06% in CF1) were the dominant active microbes at the genus level (Fig. 6 and Fig. S11 in Appendix A). The enriched *Acetobacterium wieringae*, *Acetobacterium* sp._MES1, and *Acetobacterium dehalogenans* can produce acetate from CO_2. *Wolinella* has rarely been reported in MES, based on 16S rRNA-based microbial diversity analysis [61]. However, it has been proven to be active according to the transcriptome analysis conducted in the present study. *Wolinella succinogenes* is a non-fermentative commensal rumen bacterium that can use formate or hydrogen as the electron donor in the reduction of various electron acceptors, including nitrate, nitrite, nitrous oxide, fumarate, dimethyl sulfoxide, and polysulfide [62]. Both formate and hydrogen could be easily produced in MES as the electron carriers, but the roles of *Wolinella* in carbon metabolism need to be further explored.

The expression of genes involving in the signal transduction as well as energy production and conversion were increased in the flow-electrode MES reactors. Thus, the genes involving in the energy production and conversion with fold changes ≥ 5 were compared (Figs. 6(a) and (b)). Among all these genes, the levels of genes related to ferric iron binding and oxidoreductase activity were largely changed. For example, in the AC1 sample, the highly expressed genes including COG1290, COG1969, COG2857, COG2993, COG3278, and ENOG4111TV1 served as cytochrome or cytochrome C oxidase, the highly expressed COG4659 functioned as an electron transport complex, and ENOG410Y8PW and ENOG4111UAK were involved in iron–sulfur binding. In addition, COG4656 (responsible for nitrogen fixation), COG2033 (superoxide reductase), and COG1151 (involved in reduction of hydroxylamine) were also highly expressed in AC1. Meanwhile, COG3259 (nickel-dependent hydrogenase), COG1941 (NADH ubiquinone oxidoreductase), and COG1229 (formylmethanofuran dehydrogenase) were highly expressed in CF1. A recent study has suggested that the expansion of metal ion-based cofactor pools can increase the CO_2 fixation rate of acetogen [63]. These results suggest that the flow-electrode in MES reactors can increase the relative abundance of *Acetobacterium* and the expressive abundance of genes related to energy production and conversion by promoting the expression of the genes involving in electron transfer.

Based on the KEGG functional annotation, the Wood–Ljungdahl pathway (WLP) and reductive citric acid cycle (rTCA) were found to be the pathways for carbon fixation for both the AC1 (Fig. S12 in

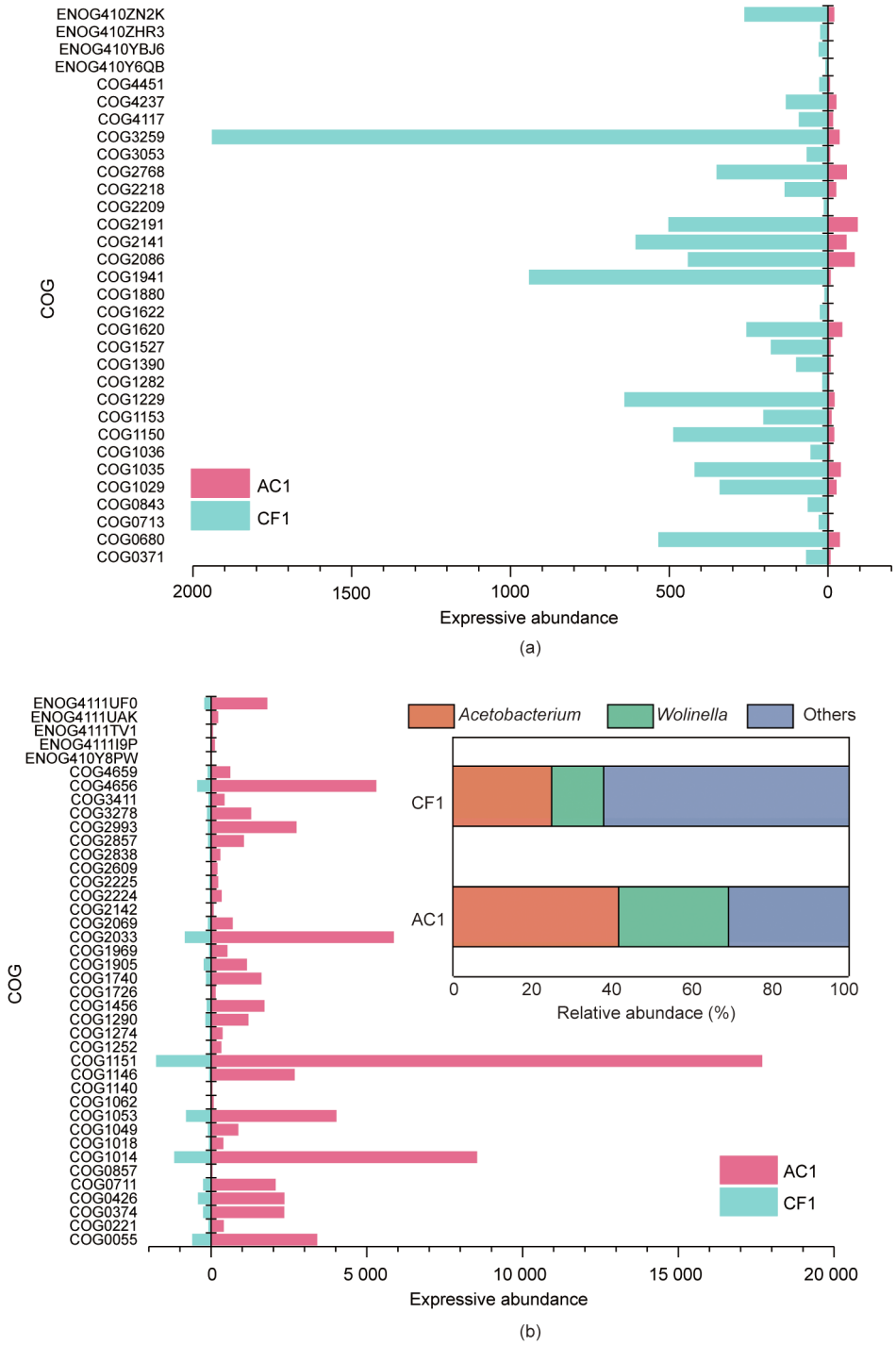

Fig. 6. Microbial community and expressive abundance of clusters of orthologous groups (COG) involving in energy production and conversion. (a) Comparison of genes with fold changes ≥ 5 in the H-type MES reactors with cathode made of carbon felt (CF1) with those in the flow-electrode MES reactor amended with powder active carbon (AC1). (b) Comparison of genes with fold change ≥ 5 in AC1 with that in CF1. The inset of (b) shows the microbial community at the genus level; sequences with the abundance of less than 5% in all samples are grouped as "others."

Appendix A) and CF1 (Fig. S13 in Appendix A). WLP is a well-known CO_2 fixation pathway of acetogens and is thought to be the main route for CO_2 bioconversion in MES reactors [64]. The rTCA takes place in Proteobacteria, Aquificae bacteria, and green sulfur bacteria [65]. In the present study, adenosine triphosphate (ATP) citrate synthase (2.3.3.8), which is responsible for electricity-driven carbon fixation, was identified in both AC1 and CF1 (Fig. S14 in Appendix A). In MES, CO_2 levels are generally high, and H_2 can be produced *in situ* through the consumption of electrons donated by cathodes; however, the roles of rTCA in carbon fixation in MES needs to be further studied [66].

3.6. Using stacked flow-electrode MES reactors to increase acetate concentration

The total electrolyte volume was 60 times greater than the electrolyte volume in the chambers. Thus, a higher volumetric productivity could be calculated by normalizing to the electrolyte

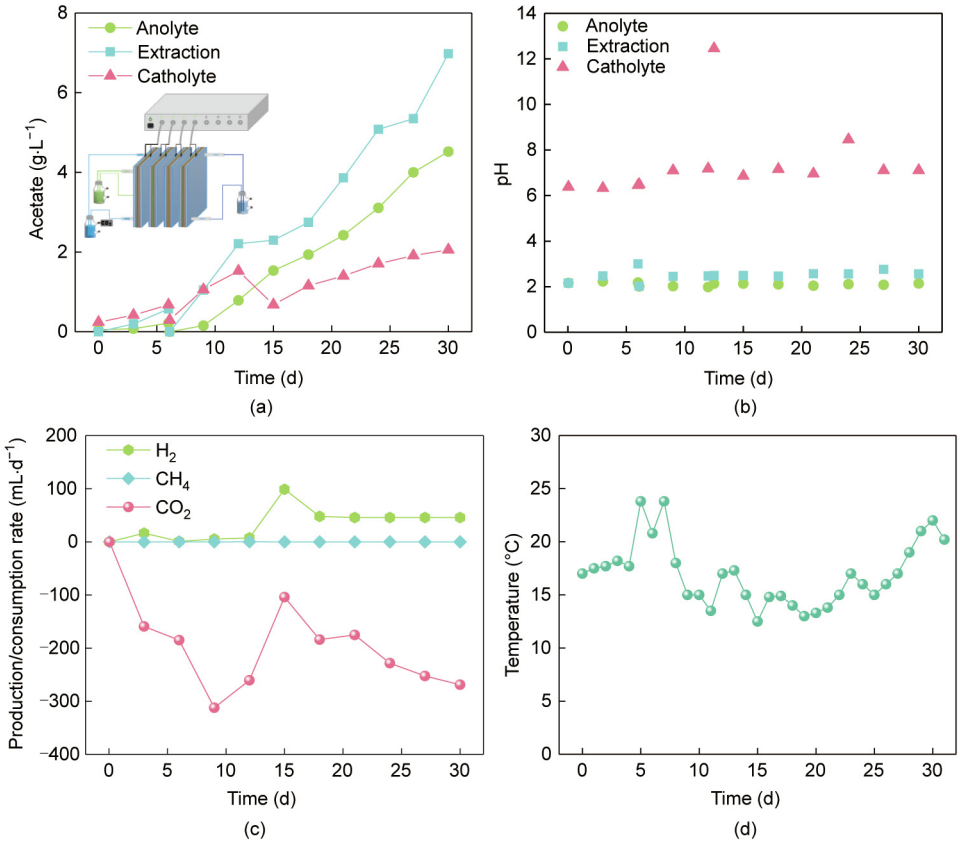

Fig. 7. (a) Performance of stacked flow-electrode MES reactors with increasing acetate concentration. (b) Time course of pH. (c) Net production and consumption of gas. (d) Fluctuation of temperature. The current was fixed at 3 mA during days 0–6, 6 mA during days 6–12, 12 mA during days 12–12.5, and 6 mA during days 12.5–30. The inset of (a) is the schematic diagram of the stacked reactors.

volume in the chambers rather than to the total electrolyte volume, as described in previous studies [67]. To increase the accumulative acetate concentration, four flow-electrode MES reactors were stacked and connected together in a series using water flow (Fig. 7(a)). Here, the concentration of acetate reached 7.0 g·L^{-1} in the extraction solution, 4.5 g·L^{-1} in the anolyte, and 2.1 g·L^{-1} in the catholyte. The stacked reactors could be steadily operated at a current of 6 mA for each reactor, but could not tolerate a current of 12 mA due to the sharp increase of pH (Fig. 7(b)). The net production and consumption of gas indicated that the bioactivity was sensitive to pH; however, it could be fully recovered when the current was decreased from 12 to 6 mA (Fig. 7(c)). In the present study, the reactors were operated at room temperature (17.3 ± 3.0) °C, and the temperatures fluctuated significantly (Fig. 7(d)).

The scale-up of the flow-electrode-based electrochemical reactors has attracted dramatically increasing interest, recently. For example, a stacked FCDI consisting of five-unit cells was constructed with hollow serpentine channels carved on both sides of the current collectors [68]. A membrane-current collector (MCC)-based FCDI could decrease the pumping energy and increase the utilization of the membrane area [69]. In addition, 3D FCDI with honeycomb-shaped lattice structures has been described to have a great potential for scale-up [70].

Temperature is important for bioconversion, and almost all studies on MES that have been reported thus far were performed under mesophilic temperatures, which range from 25 to 35 °C [58]. However, a recent report has investigated the use of thermophilic MES reactors for the production of acetate and polyhydroxybutyrate (PHB) at 50 and 60 °C, respectively [58,71]. According to the report, as the temperature decrease, the activity in MES should decrease and should be dependent on the abundance of the enriched microbial community [72].

In the present study, a gas bag was connected to the MES reactors to allow the passive supplement of CO_2. Hence, the competitiveness of MES was partially restricted by the limited CO_2 mass transfer, which occurred at much larger current densities [51,73]. To address this CO_2 mass transfer limitation, the cathode chamber is continuously purged with CO_2 along with bicarbonate in media [74]. In addition, reactors with novel configurations such as porous Ni-hollow fiber membrane cathodes and gas diffusion cathodes with optimized CO_2 concentration and bubble sizes, have been shown to also be beneficial to enhancing CO_2 mass transfer in MES [22,51,75]. Concentrations of CO_2 and bicarbonate in the catholyte are highly dependent on temperature, pH, and salinity [73,76,77]. These results suggest that the performance of the flow-electrode MES reactors can be further improved by optimizing the setup configurations and/or environmental parameters.

4. Conclusions

In summary, a novel flow-electrode MES reactor was constructed for the first time to increase acetate production and decrease energy consumption. For the acetate production in the flow-electrode MES reactors, an acetate production rate of (16 ± 1) g·m^{-2}·d^{-1} was obtained with an energy consumption of (0.020 ± 0.005) kW·h·g^{-1} and an energy efficiency of 18.7% ± 1.3%. In addition, the Coulombic efficiency of acetate and total soluble chemicals were 43.5% ± 3.1% and 50.8% ± 8.4%, respectively. The

use of the flow-electrode decreased the net water flux rate and charge transfer resistance, while had little impact on the cell voltage, rheological behavior, and acetate adsorption. *Acetobacterium* and *Wolinella* were the dominant microbes, while WLP and rTCA were the pathways that the microbes utilized for carbon fixation. The utilization of the flow-electrode MES enhanced the expressive abundance of genes responsible for energy production and conversion. Concentration of acetate in the stacked flow-electrode MES reactors reached 7.0 $g{\cdot}L^{-1}$. Further studies should be carried out in order to expand the product spectrum in the flow-electrode MES reactors.

Acknowledgments

This work was supported by the National Natural Science Foundation of China (51908131) and the Natural Science Foundation of Fujian Province (2020J01563).

Compliance with ethics guidelines

Na Chu, Donglin Wang, Houfeng Wang, Qinjun Liang, Jiali Chang, Yu Gao, Yong Jiang, and Raymond Jianxiong Zeng declare that they have no conflict of interest or financial conflicts to disclose.

Appendix A. Supplementary data

Supplementary data to this article can be found online at https://doi.org/10.1016/j.eng.2021.09.015.

References

[1] Zhou L, Wang H, Zhang Z, Zhang J, Chen H, Bi X, et al. Novel perspective for urban water resource management: 5R generation. Front Environ Sci Eng 2021;15(1):16.
[2] Hu G, Chen C, Lu HT, Wu Y, Liu C, Tao L, et al. A review of technical advances, barriers, and solutions in the power to hydrogen (P2H) roadmap. Engineering 2020;6(12):1364–80.
[3] Huang Z, Grim RG, Schaidle JA, Tao L. The economic outlook for converting CO_2 and electrons to molecules. Energy Environ Sci 2021;14(7):3664–78.
[4] Zhang Z, Pan SY, Li H, Cai J, Olabi AG, Anthony EJ, et al. Recent advances in carbon dioxide utilization. Renew Sustain Energy Rev 2020;125:109799.
[5] Grim RG, Huang Z, Guarnieri MT, Ferrell JR, Tao L, Schaidle JA. Transforming the carbon economy: challenges and opportunities in the convergence of low-cost electricity and reductive CO_2 utilization. Energy Environ Sci 2020;13(2):472–94.
[6] Greig C. Getting to net-zero emissions. Engineering 2020;6(12):1341–2.
[7] Dessì P, Rovira-Alsina L, Sánchez C, Dinesh GK, Tong W, Chatterjee P, et al. Microbial electrosynthesis: towards sustainable biorefineries for production of green chemicals from CO_2 emissions. Biotechnol Adv 2021;46:107675.
[8] Flexer V, Jourdin L. Purposely designed hierarchical porous electrodes for high rate microbial electrosynthesis of acetate from carbon dioxide. Acc Chem Res 2020;53(2):311–21.
[9] Jiang Y, Liang Q, Chu N, Hao W, Zhang L, Zhan G, et al. A slurry electrode integrated with membrane electrolysis for high-performance acetate production in microbial electrosynthesis. Sci Total Environ 2020;741:140198.
[10] Kim Y, Lama S, Agrawal D, Kumar V, Park S. Acetate as a potential feedstock for the production of value-added chemicals: metabolism and applications. Biotechnol Adv 2021;49:107736.
[11] LaBelle EV, Marshall CW, May HD. Microbiome for the electrosynthesis of chemicals from carbon dioxide. Acc Chem Res 2020;53(1):62–71.
[12] Chu N, Liang Q, Jiang Y, Zeng RJ. Microbial electrochemical platform for the production of renewable fuels and chemicals. Biosens Bioelectron 2020;150:111922.
[13] Chu N, Hao W, Wu Q, Liang Q, Jiang Y, Ren JZ, et al. Microbial electrosynthesis for producing medium chain fatty acids. Engineering 2022;16:141–53.
[14] Zeng AP. New bioproduction systems for chemicals and fuels: needs and new development. Biotechnol Adv 2019;37(4):508–18.
[15] Liang P, Duan R, Jiang Y, Zhang X, Qiu Y, Huang X. One-year operation of 1000-L modularized microbial fuel cell for municipal wastewater treatment. Water Res 2018;141:1–8.
[16] Quejigo JR, Korth B, Kuchenbuch A, Harnisch F. Redox potential heterogeneity in fixed-bed electrodes leads to microbial stratification and inhomogeneous performance. ChemSusChem 2021;14(4):1155–65.
[17] Jourdin L, Burdyny T. Microbial electrosynthesis: where do we go from here? Trends Biotechnol 2021;39(4):359–69.
[18] Ma J, Ma J, Zhang C, Song J, Dong W, Waite TD. Flow-electrode capacitive deionization (FCDI) scale-up using a membrane stack configuration. Water Res 2020;168:115186.
[19] Mourshed M, Niya SMR, Ojha R, Rosengarten G, Andrews J, Shabani B. Carbon-based slurry electrodes for energy storage and power supply systems. Energy Storage Mater 2021;40:461–89.
[20] Yang F, He Y, Rosentsvit L, Suss ME, Zhang X, Gao T, et al. Flow-electrode capacitive deionization: a review and new perspectives. Water Res 2021;200:117222.
[21] Claassens NJ, Cotton CAR, Kopljar D, Bar-Even A. Making quantitative sense of electromicrobial production. Nat Catal 2019;2(5):437–47.
[22] Bajracharya S, Vanbroekhoven K, Buisman CJN, Strik DPBTB, Pant D. Bioelectrochemical conversion of CO_2 to chemicals: CO_2 as a next generation feedstock for electricity-driven bioproduction in batch and continuous modes. Faraday Discuss 2017;202:433–49.
[23] Jiang Y, Chu N, Zeng RJ. Submersible probe type microbial electrochemical sensor for volatile fatty acids monitoring in the anaerobic digestion process. J Clean Prod 2019;232:1371–8.
[24] Yang F, Ma J, Zhang X, Huang X, Liang P. Decreased charge transport distance by titanium mesh-membrane assembly for flow-electrode capacitive deionization with high desalination performance. Water Res 2019;164:114904.
[25] Jiang Y, Chu Na, Zhang W, Ma J, Zhang F, Liang P, et al. Zinc: a promising material for electrocatalyst-assisted microbial electrosynthesis of carboxylic acids from carbon dioxide. Water Res 2019;159:87–94.
[26] Izadi P, Fontmorin JM, Godain A, Yu EH, Head IM. Parameters influencing the development of highly conductive and efficient biofilm during microbial electrosynthesis: the importance of applied potential and inorganic carbon source. NPJ Biofilms Microbiomes 2020;6(1):40.
[27] Chen H, Dong F, Minteer SD. The progress and outlook of bioelectrocatalysis for the production of chemicals, fuels and materials. Nat Catal 2020;3(3):225–44.
[28] Wang L, Yang C, Thangavel S, Guo Z, Chen C, Wang A, et al. Enhanced hydrogen production in microbial electrolysis through strategies of carbon recovery from alkaline/thermal treated sludge. Front Environ Sci Eng 2021;15(4):56.
[29] Liang Q, Gao Y, Li Z, Cai J, Chu N, Hao W, et al. Electricity-driven ammonia oxidation and acetate production in microbial electrosynthesis systems. Front Environ Sci Eng 2022;16(4):42.
[30] Wu S, Li H, Zhou X, Liang P, Zhang X, Jiang Y, et al. A novel pilot-scale stacked microbial fuel cell for efficient electricity generation and wastewater treatment. Water Res 2016;98:396–403.
[31] Wang HF, Hu H, Yang HY, Zeng RJ. Characterization of anaerobic granular sludge using a rheological approach. Water Res 2016;106:116–25.
[32] Ma J, Liang P, Sun X, Zhang H, Bian Y, Yang F, et al. Energy recovery from the flow-electrode capacitive deionization. J Power Sources 2019;421:50–5.
[33] Jiang Y, Su M, Zhang Y, Zhan G, Tao Y, Li D. Bioelectrochemical systems for simultaneously production of methane and acetate from carbon dioxide at relatively high rate. Int J Hydrogen Energy 2013;38(8):3497–502.
[34] LaBelle EV, May HD. Energy efficiency and productivity enhancement of microbial electrosynthesis of acetate. Front Microbiol 2017;8:756.
[35] Zhang X, Zhang D, Huang Y, Wu S, Lu P. The anodic potential shaped a cryptic sulfur cycling with forming thiosulfate in a microbial fuel cell treating hydraulic fracturing flowback water. Water Res 2020;185:116270.
[36] Hyatt D, Chen GL, Locascio PF, Land ML, Larimer FW, Hauser LJ. Prodigal: prokaryotic gene recognition and translation initiation site identification. BMC Bioinf 2010;11(1):119.
[37] Fu L, Niu B, Zhu Z, Wu S, Li W. CD-HIT: accelerated for clustering the next-generation sequencing data. Bioinformatics 2012;28(23):3150–2.
[38] Huerta-Cepas J, Szklarczyk D, Heller D, Hernández-Plaza A, Forslund SK, Cook H, et al. eggNOG 5.0: a hierarchical, functionally and phylogenetically annotated orthology resource based on 5090 organisms and 2502 viruses. Nucleic Acids Res 2019;47(D1):D309–14.
[39] Jiang Y, Chu N, Qian DK, Zeng RJ. Microbial electrochemical stimulation of caproate production from ethanol and carbon dioxide. Bioresour Technol 2020;295:122266.
[40] Chen H, Simoska O, Lim K, Grattieri M, Yuan M, Dong F, et al. Fundamentals, applications, and future directions of bioelectrocatalysis. Chem Rev 2020;120(23):12903–93.
[41] Gildemyn S, Verbeeck K, Slabbinck R, Andersen SJ, Prévoteau A, Rabaey K. Integrated production, extraction, and concentration of acetic acid from CO_2 through microbial electrosynthesis. Environ Sci Technol Lett 2015;2(11):325–8.
[42] Chu Na, Liang Q, Zhang W, Ge Z, Hao W, Jiang Y, et al. Waste C1 gases as alternatives to pure CO_2 improved the microbial electrosynthesis of C4 and C6 carboxylates. ACS Sustain Chem Eng 2020;8(23):8773–82.
[43] Mohanakrishna G, Vanbroekhoven K, Pant D. Imperative role of applied potential and inorganic carbon source on acetate production through microbial electrosynthesis. J CO_2 Util 2016;15:57–64.
[44] Jiang Y, May HD, Lu L, Liang P, Huang X, Ren ZJ. Carbon dioxide and organic waste valorization by microbial electrosynthesis and electro-fermentation. Water Res 2019;149:42–55.
[45] Patil SA, Arends JBA, Vanwonterghem I, van Meerbergen J, Guo K, Tyson GW, et al. Selective enrichment establishes a stable performing community for microbial electrosynthesis of acetate from CO_2. Environ Sci Technol 2015;49(14):8833–43.

[46] Xiang Y, Liu G, Zhang R, Lu Y, Luo H. High-efficient acetate production from carbon dioxide using a bioanode microbial electrosynthesis system with bipolar membrane. Bioresour Technol 2017;233:227–35.
[47] Roy M, Yadav R, Chiranjeevi P, Patil SA. Direct utilization of industrial carbon dioxide with low impurities for acetate production via microbial electrosynthesis. Bioresour Technol 2021;320(Pt A):124289.
[48] Aryal N, Ammam F, Patil SA, Pant D. An overview of cathode materials for microbial electrosynthesis of chemicals from carbon dioxide. Green Chem 2017;19(24):5748–60.
[49] Jourdin L, Grieger T, Monetti J, Flexer V, Freguia S, Lu Y, et al. High acetic acid production rate obtained by microbial electrosynthesis from carbon dioxide. Environ Sci Technol 2015;49(22):13566–74.
[50] Jourdin L, Freguia S, Flexer V, Keller J. Bringing high-rate, CO_2-based microbial electrosynthesis closer to practical implementation through improved electrode design and operating conditions. Environ Sci Technol 2016;50 (4):1982–9.
[51] Bian B, Bajracharya S, Xu J, Pant D, Saikaly PE. Microbial electrosynthesis from CO_2: challenges, opportunities and perspectives in the context of circular bioeconomy. Bioresour Technol 2020;302:122863.
[52] Park SG, Rhee C, Shin SG, Shin J, Mohamed HO, Choi YJ, et al. Methanogenesis stimulation and inhibition for the production of different target electrobiofuels in microbial electrolysis cells through an on-demand control strategy using the coenzyme M and 2-bromoethanesulfonate. Environ Int 2019;131: 105006.
[53] Nevin KP, Woodard TL, Franks AE, Summers ZM, Lovley DR, Colwell RR. Microbial electrosynthesis: feeding microbes electricity to convert carbon dioxide and water to multicarbon extracellular organic compounds. mBio 2010;1(2):e00103-10.
[54] Satinover SJ, Schell D, Borole AP. Achieving high hydrogen productivities of 20 L/L-day via microbial electrolysis of corn stover fermentation products. Appl Energy 2020;259:114126.
[55] Gildemyn S, Verbeeck K, Jansen R, Rabaey K. The type of ion selective membrane determines stability and production levels of microbial electrosynthesis. Bioresour Technol 2017;224:358–64.
[56] Bian Y, Yang X, Liang P, Jiang Y, Zhang C, Huang X. Enhanced desalination performance of membrane capacitive deionization cells by packing the flow chamber with granular activated carbon. Water Res 2015;85:371–6.
[57] Ma J, Ma J, Zhang C, Song J, Collins RN, Waite TD. Water recovery rate in short-circuited closed-cycle operation of flow-electrode capacitive deionization (FCDI). Environ Sci Technol 2019;53(23):13859–67.
[58] Reiner JE, Geiger K, Hackbarth M, Fink M, Lapp CJ, Jung T, et al. From an extremophilic community to an electroautotrophic production strain: identifying a novel *Knallgas* bacterium as cathodic biofilm biocatalyst. ISME J 2020;14(5):1125–40.
[59] Jiang Y, Zeng RJ. Expanding the product spectrum of value added chemicals in microbial electrosynthesis through integrated process design—a review. Bioresour Technol 2018;269:503–12.
[60] Vassilev I, Hernandez PA, Batlle-Vilanova P, Freguia S, Krömer JO, Keller J, et al. Microbial electrosynthesis of isobutyric, butyric, caproic acids, and corresponding alcohols from carbon dioxide. ACS Sustain Chem Eng 2018;6 (7):8485–93.
[61] Logan BE, Rossi R, Ragab A, Saikaly PE. Electroactive microorganisms in bioelectrochemical systems. Nat Rev Microbiol 2019;17(5):307–19.
[62] Hein S, Witt S, Simon J. Clade II nitrous oxide respiration of Wolinella succinogenes depends on the NosG, -C1, -C2, -H electron transport module, NosB and a Rieske/cytochrome bc complex. Environ Microbiol 2017;19 (12):4913–25.
[63] Jin S, Jeon Y, Jeon MS, Shin J, Song Y, Kang S, et al. Acetogenic bacteria utilize light-driven electrons as an energy source for autotrophic growth. Proc Natl Acad Sci USA 2021;118(9): e2020552118.
[64] Müller V. New horizons in acetogenic conversion of one-carbon substrates and biological hydrogen storage. Trends Biotechnol 2019;37(12):1344–54.
[65] Liu Z, Wang K, Chen Y, Tan T, Nielsen J. Third-generation biorefineries as the means to produce fuels and chemicals from CO_2. Nat Catal 2020;3 (3):274–88.
[66] Steffens L, Pettinato E, Steiner TM, Mall A, König S, Eisenreich W, et al. High CO_2 levels drive the TCA cycle backwards towards autotrophy. Nature 2021;592(7856):784–8.
[67] Jourdin L, Winkelhorst M, Rawls B, Buisman CJN, Strik DPBTB. Enhanced selectivity to butyrate and caproate above acetate in continuous bioelectrochemical chain elongation from CO_2: steering with CO_2 loading rate and hydraulic retention time. Bioresource Technol Rep 2019;7:100284.
[68] Yang S, Jeon S, Kim H, Choi J, Yeo J, Park H, et al. Stack design and operation for scaling up the capacity of flow-electrode capacitive deionization technology. ACS Sustain Chem Eng 2016;4(8):4174–80.
[69] Xu L, Mao Y, Zong Y, Wu D. Scale-up desalination: membrane-current collector assembly in flow-electrode capacitive deionization system. Water Res 2021;190:116782.
[70] Cho Y, Lee KS, Yang S, Choi J, Park H, Kim DK. A novel three-dimensional desalination system utilizing honeycomb-shaped lattice structures for flow-electrode capacitive deionization. Energy Environ Sci 2017;10(8):1746–50.
[71] Rovira-Alsina L, Perona-Vico E, Bañeras L, Colprim J, Balaguer MD, Puig S. Thermophilic bio-electro CO_2 recycling into organic compounds. Green Chem 2020;22(9):2947–55.
[72] Yang HY, Hou NN, Wang YX, Liu J, He CS, Wang YR, et al. Mixed-culture biocathodes for acetate production from CO_2 reduction in the microbial electrosynthesis: impact of temperature. Sci Total Environ 2021;790:148128.
[73] Prévoteau A, Carvajal-Arroyo JM, Ganigué R, Rabaey K. Microbial electrosynthesis from CO_2: forever a promise? Curr Opin Biotechnol 2020;62:48–57.
[74] Ameen F, Alshehri WA, Nadhari SA. Effect of electroactive biofilm formation on acetic acid production in anaerobic sludge driven microbial electrosynthesis. ACS Sustain Chem Eng 2020;8(1):311–8.
[75] Fontmorin JM, Izadi P, Li D, Lim SS, Farooq S, Bilal SS, et al. Gas diffusion electrodes modified with binary doped polyaniline for enhanced CO_2 conversion during microbial electrosynthesis. Electrochim Acta 2021;372:137853.
[76] Zhang S, Jiang J, Wang H, Li F, Hua T, Wang W. A review of microbial electrosynthesis applied to carbon dioxide capture and conversion: the basic principles, electrode materials, and bioproducts. J CO_2 Util 2021;51:101640.
[77] Gao T, Zhang H, Xu X, Teng J. Integrating microbial electrolysis cell based on electrochemical carbon dioxide reduction into anaerobic osmosis membrane reactor for biogas upgrading. Water Res 2021;190:116679.